Correa et al. Genome Biology (2016) 17:125
DOI 10.1186/s13059-016-0990-4

Genome Biology

RESEARCH Open Access

Functional genomics analyses of RNA-binding proteins reveal the splicing regulator SNRPB as an oncogenic candidate in glioblastoma

Bruna R. Correa[1,2], Patricia Rosa de Araujo[2], Mei Qiao[2], Suzanne C. Burns[2], Chen Chen[3], Richard Schlegel[3], Seema Agarwal[3], Pedro A. F. Galante[1*] and Luiz O. F. Penalva[2,4*]

Abstract

Background: Glioblastoma (GBM) is the most common and aggressive type of brain tumor. Currently, GBM has an extremely poor outcome and there is no effective treatment. In this context, genomic and transcriptomic analyses have become important tools to identify new avenues for therapies. RNA-binding proteins (RBPs) are master regulators of co- and post-transcriptional events; however, their role in GBM remains poorly understood. To further our knowledge of novel regulatory pathways that could contribute to gliomagenesis, we have conducted a systematic study of RBPs in GBM.

Results: By measuring expression levels of 1542 human RBPs in GBM samples and glioma stem cell samples, we identified 58 consistently upregulated RBPs. Survival analysis revealed that increased expression of 21 RBPs was also associated with a poor prognosis. To assess the functional impact of those RBPs, we modulated their expression in GBM cell lines and performed viability, proliferation, and apoptosis assays. Combined results revealed a prominent oncogenic candidate, *SNRPB*, which encodes core spliceosome machinery components. To reveal the impact of SNRPB on splicing and gene expression, we performed its knockdown in a GBM cell line followed by RNA sequencing. We found that the affected genes were involved in RNA processing, DNA repair, and chromatin remodeling. Additionally, genes and pathways already associated with gliomagenesis, as well as a set of general cancer genes, also presented with splicing and expression alterations.

Conclusions: Our study provides new insights into how RBPs, and specifically SNRPB, regulate gene expression and directly impact GBM development.

Keywords: RNA-binding proteins, Glioblastoma, Glioma stem cells, SNRPB, Splicing

Background

Glioblastoma (GBM) is the most common and lethal tumor type of the central nervous system, with 16,000 new cases per year in the US alone [1]. GBM is highly heterogenic, invasive, and refractory to the current standard of care, which is a combination of surgical resection, adjuvant radiotherapy, and temozolomide [2]. Despite decades of research, the overall outcome for patients with GBM remains extremely poor, with an average survival of approximately 15 months after diagnosis [1, 3–5].

To identify new targets for therapy, The Cancer Genome Atlas (TCGA) consortium produced a comprehensive somatic landscape of GBM through a set of genomic, epigenomic, transcriptomic, and proteomic analyses, combining molecular and clinical data for 543 patients [6, 7]. These analyses have improved our understanding of GBM pathobiology, emphasizing that gliomagenesis is driven by signaling networks with functional redundancy, which allows adaptation in response to therapy. Because novel therapeutic strategies based on these findings have not yet

* Correspondence: pgalante@mochsl.org.br; penalva@uthscsa.edu
[1]Centro de Oncologia Molecular, Hospital Sírio-Libanês, São Paulo, Brazil
[2]Children's Cancer Research Institute, UTHSCSA, San Antonio, TX, USA
Full list of author information is available at the end of the article

become a reality, it is necessary to investigate additional pathways of gene deregulation in GBM. Equally important is the study of glioma stem cells (GSCs), which are particularly relevant to tumor initiation and resistance to treatment [8–10]. Unveiling individual genes and pathways that contribute to GSC survival and phenotype maintenance might enable the design of novel therapeutic strategies against GBM.

RNA-binding proteins (RBPs) are master regulators of co- and post-transcriptional mechanisms, including RNA processing (splicing, capping, and polyadenylation), transport, decay, localization, and translation. They are still a poorly characterized class of regulators, with hundreds of new members only recently identified via novel experimental high-throughput approaches [11–13]. The most updated human RBP catalog includes 1542 genes [14], which represents ~7.5 % of human coding genes (GENCODE version 19 [15]). Mutations and alterations in RBP expression levels, which have been observed in many tumor tissues [16–18], are known to impact large gene sets and to contribute to tumor initiation and growth. In fact, numerous well-characterized RBPs such as HuR, Musashi1, Sam68, and eIF4E have been implicated in multiple tumor types [19–22]. In the context of neural tissue, the number of tissue-specific RBPs and alternative splicing isoforms is particularly high compared with other tissues [14, 23–25]. Hence, RBPs play key roles in this biological context and their alteration is expected to be a major contributor to gliomagenesis. Some important players include Musashi1 [26–28], HuR [27], hnRNP proteins (H and A2/B1) [29–32], and PTB [29, 33, 34].

In order to identify novel RBPs potentially implicated in GBM development, we conducted a combination of transcriptomic analyses followed by functional screenings. We found 58 genes with oncogenic potential, defined as those with high expression in GBM and GSC samples relative to their normal counterparts. Twenty-one of these genes are also associated with a poor prognosis and were further selected for functional analyses. *SNRPB*, which encodes core components of the spliceosome complex SmB/B', showed the strongest impact on viability, proliferation, and apoptosis. We determined that changes in SNRPB expression levels have a large impact on expression and splicing regulation and preferentially affect alternative exons and introns. RNA processing, DNA repair, and chromatin remodeling are among the biological processes with the highest number of genes affected by SNRPB at expression and splicing levels. Moreover, several genes in pathways relevant to GBM initiation and development, such as *RTK*, *PI3K*, *RAS*, *MAPK*, *AKT*, *RB*, and *p53*, as well as a set of additional cancer genes, displayed alterations in their splicing and expression profiles upon *SNRPB* knockdown.

Results

Several RBPs are aberrantly expressed in GBM and GSCs

To identify RBPs potentially involved in GBM development, we examined the expression profiles of all 1542 human catalogued RBP coding genes [14] in two different contexts: GBM samples from TCGA versus normal brain; and GSCs versus normal neural progenitor cells (Fig. 1a). We obtained raw RNA sequencing (RNA-Seq) data for 170 GBM samples from TCGA database (Additional file 1: Table S1) and compared them with 14 normal brain samples: eight samples from two studies available in the Sequence Read Archive (SRA), one sample from the Human Body Map, and five samples from TCGA (see 'Methods'; Additional file 1: Table S1). This approach allowed the identification of 223 upregulated and 135 downregulated RBPs in tumors compared to normal samples (Fig. 1b top panel; Additional file 1: Table S2). Next, we looked at the expression of these differentially expressed RBPs, classifying all samples according to the four molecular GBM subtypes (classical, neural, proneural, and mesenchymal) to identify particular associations (if any). Results indicated that the overall expression profile was very similar among subtypes, with no differentially expressed RBPs showing drastic changes across subtypes (Additional file 2: Figure S1).

GSCs constitute a unique subpopulation within the tumor and display features similar to normal stem cells [35]. Their association with tumor relapse is often linked to their tumor-initiating capacity as well as radio- and chemoresistance [35–38]. Therefore, identifying regulators that maintain GSC phenotypes and/or contribute to their survival is critical for designing novel therapeutic strategies. We examined the microarray dataset of Mao et al. [39] to identify differentially expressed RBPs in GSCs in comparison to normal neural progenitor cells. This analysis revealed a total of 275 upregulated and 85 downregulated RBPs in GSCs (Fig. 1b bottom panel; Additional file 1: Table S3).

We focused next on the identification of "pro-oncogenic RBPs." We selected these RBPs because they tend to be more attractive targets in therapeutic contexts [40] and they are easier to handle in screening studies [41]. Results from both transcriptomic studies were merged: 58 genes were determined to be upregulated in both GBM and GSC samples (Fig. 1c), which represents a highly significant overlap (p-value = 0.0006; hypergeometric test). Those 58 genes were selected for further analyses.

Upregulation of RBPs is associated with decreased survival and is prevalent in higher grade gliomas

To determine whether our set of 58 pro-oncogenic RBPs exhibits an association with poor prognosis in gliomas,

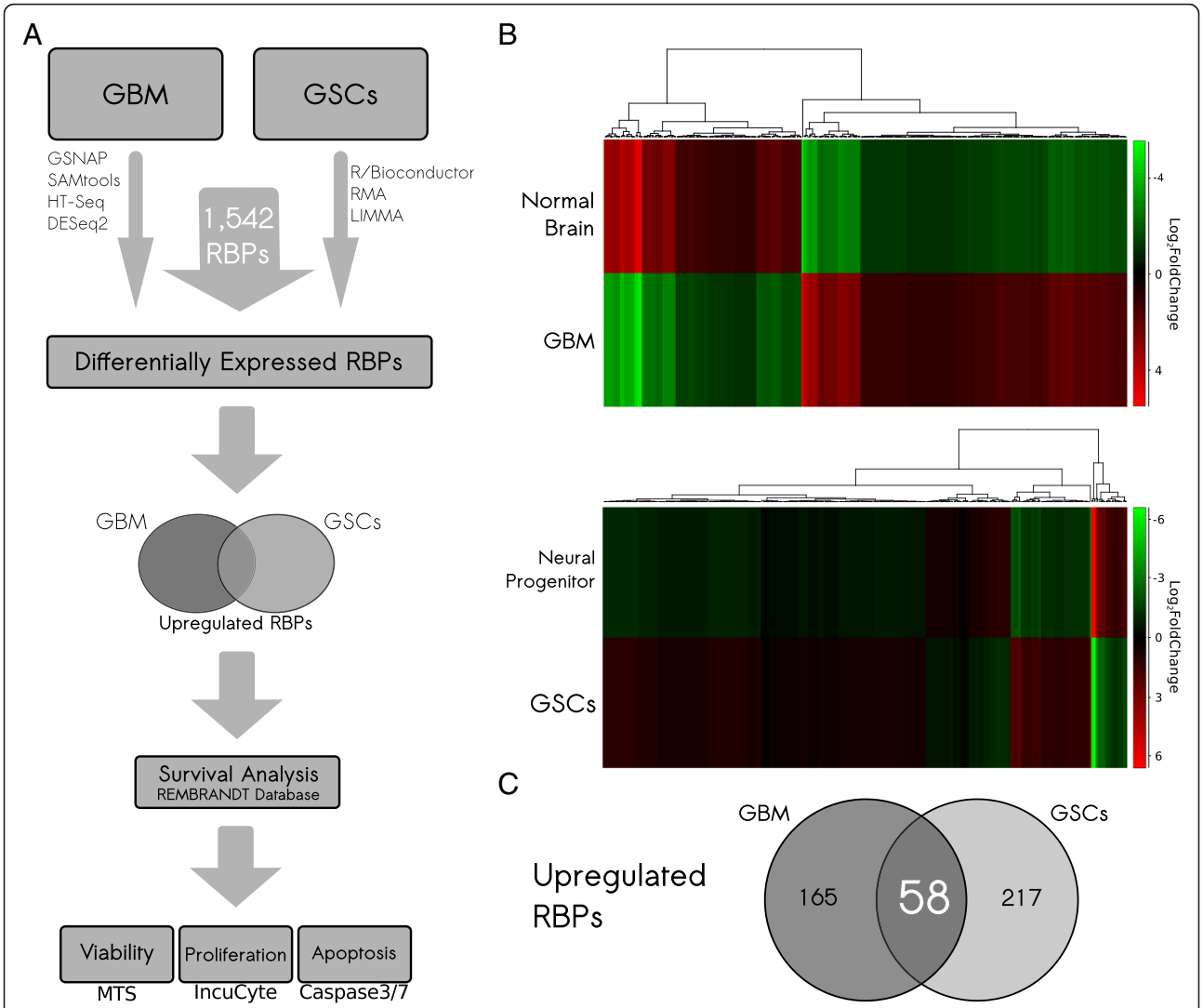

Fig. 1 Experimental design and RNA-binding protein (*RBP*) expression profile in glioblastoma (*GBM*) and glioma stem cells (*GSCs*). **a** Gene expression results from GBM and GSC samples were combined to identify upregulated RBPs. Those RBPs were evaluated regarding their association with survival decrease, and their functional impact in GBM was assayed by a set of functional assays. **b** Heatmaps show all differentially expressed RBPs in GBM samples from The Cancer Genome Atlas compared to normal brain samples and in GSC samples compared to a normal neural progenitor cell line. **c** Venn diagram shows the intersection between gene expression analyses

we used clinical and expression data from the REMBRANDT database [42]. We built Kaplan-Meier survival curves comparing samples with increased expression of the selected RBPs to all other samples. Twenty-one out of the 58 upregulated RBPs showed an association with survival reduction when overexpressed (p-value < 0.05; log-rank test; Additional file 2: Figure S2). Figure 2a presents a summary of the selected RBPs and their results in survival analysis.

We also evaluated gene expression levels of these RBPs using a large cohort of normal brain samples generated by the Genotype-Tissue Expression (GTEx) Project [43]. By comparing expression levels of the 21 RBPs in 222 normal brain samples from GTEx with 170 GBM samples from TCGA, we were able to confirm the overexpression of our selected RBPs in GBM samples (Additional file 1: Table S4).

Finally, to corroborate the relevance of these 21 selected RBPs in an additional context, we evaluated their expression levels in 167 GBM samples (grade IV glioma) versus 218 lower grade glioma samples (grades II and III astrocytomas and oligodendrogliomas) from TCGA. In general, analyzed RBPs exhibited higher expression levels in GBM samples than in lower grade glioma samples (p-value < 0.001; Wilcoxon rank-sum test; Fig. 2b; Additional file 1: Table S5). The only exception was RNASET2, which presented no significant difference in one comparison (p-value = 0.1428 for GBMs versus

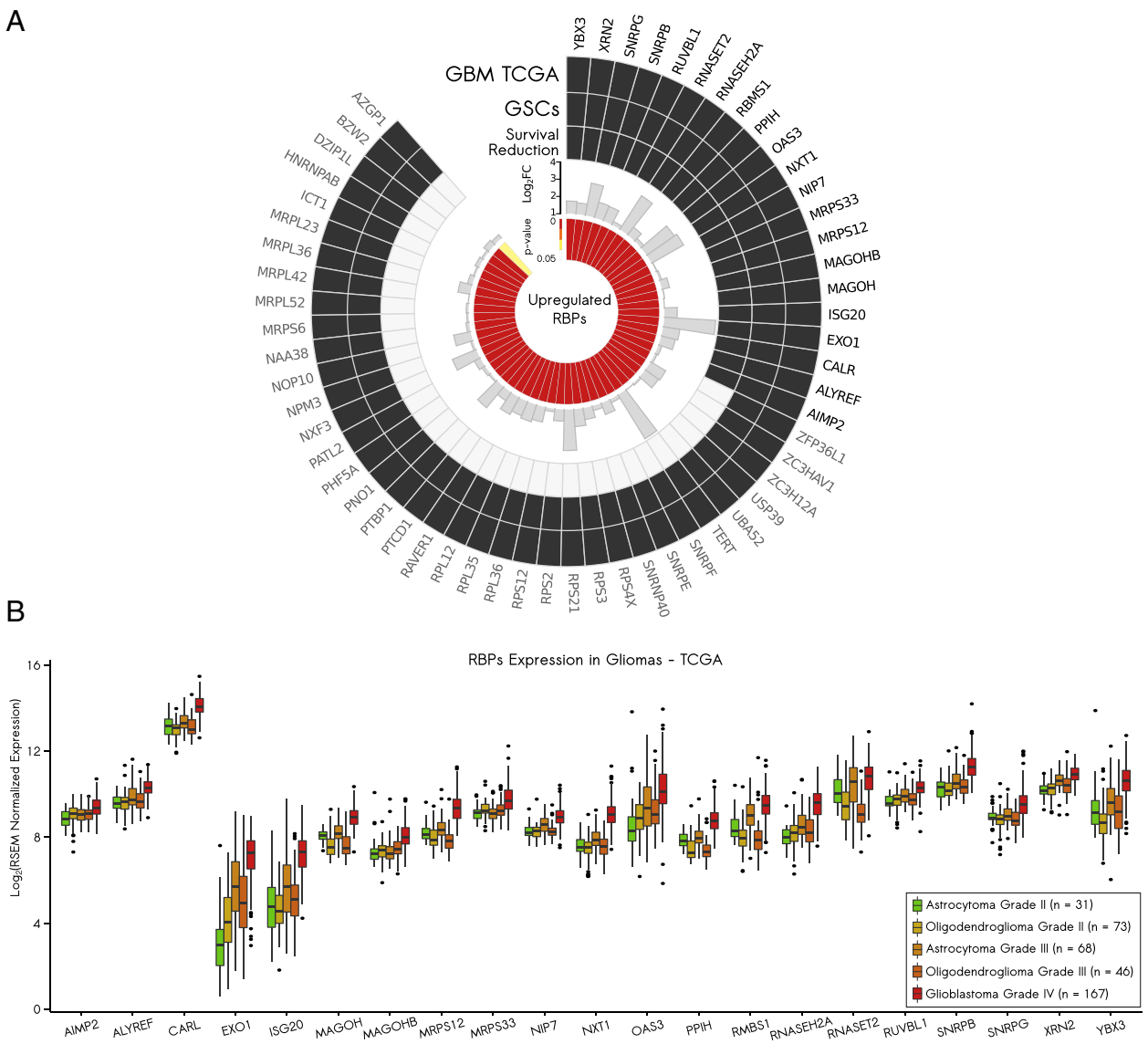

Fig. 2 Candidates' selection and characterization. **a** Circos plot shows 58 upregulated RNA-binding proteins (*RBPs*) in glioblastoma (*GBM*) samples from The Cancer Genome Atlas (*TCGA*) and glioma stem cell (*GSC*) lines. Fold-changes and corrected *p*-values were extracted from the RNA-Seq analysis (*GBM TCGA*). Twenty-one RBPs were also associated with survival reduction and were further investigated. **b** RBPs exhibited higher expression levels in GBMs compared with lower grade gliomas

grade III astrocytomas; Wilcoxon rank-sum test; Fig. 2b; Additional file 1: Table S5).

Analysis of regulatory elements potentially triggering overexpression of RBPs in GBM

To try to identify mechanisms responsible for the upregulation of RBPs in tumor samples, we evaluated whether the 21 selected RBPs are targeted by frequently downregulated miRNAs in GBM (tumor suppressor miRNAs). Using a list of tumor suppressor miRNAs compiled by Hermansen and Kristensen [44], we found that 18 of those miRNAs potentially target 15 out of the 21 RBPs. We observed a significant enrichment for miR-124, which presented the highest number of targets: six RBPs in total (p-value = 0.0099; hypergeometric test; Additional file 2: Figure S3).

We also evaluated whether the 21 RBPs presented mutations and/or copy-number alterations (CNA) in GBM samples from TCGA. We analyzed 273 GBM samples with exome sequencing and CNA data available in cBioPortal [45, 46]. Only 10 % of the samples displayed alterations in at least one of our selected RBPs. CNA, missense mutations, and/or truncating mutations were present in 17 out of 21 evaluated RBPs, not different from

randomly selected RBPs sets (p-value > 0.1; simulation with 100,000 sets of 21 randomly selected RBPs; Additional file 2: Figure S4).

RBPs impact cellular viability, proliferation, and apoptosis in GBM

The 21 selected RBPs were then evaluated in a functional screening. Transient knockdowns were performed with siRNAs (median knockdown efficiency ~90 %; Additional file 1: Table S6) in U251 and U343 GBM cells and their impact on viability (MTS assay), proliferation (IncuCyte), and apoptosis (Caspase-3/7 assay) were evaluated. Results of these three assays are summarized in Table 1 and represented in Additional file 2: Figures S5–S7. Out of the 21 investigated RBPs, 15 showed significant effect in at least one assay in one or both cell lines.

SNRPB as a potential new oncogenic candidate in GBM

Overall, *SNRPB*, which encodes core spliceosome components SmB/B', exhibited the most consistent results in the functional screening: knockdown of this gene decreased viability (Fig. 3a), increased apoptosis (Fig. 3b), and decreased proliferation (Fig. 3c) in both U251 and U343 cell lines.

We conducted additional experiments to determine the impact of *SNRPB* on the growth of GSC cultures. Lines 326 and 83 were described in a previous study [39]. We knocked down the expression of *SNRPB* in these two GSC lines grown as conditionally reprogrammed cells (CRCs). CRCs have been shown to better recapitulate the characteristics of original tumor cells [47]. In both cell lines, *SNRPB* knockdown led to inhibition of cell growth and to cell detachment (Fig. 3d). Additionally, because GBMs are known to be highly undifferentiated tumors [48], we checked *SNRPB* expression in mouse neural stem cells versus differentiated neural cells and determined that *SNRPB* expression was higher in undifferentiated cells (Fig. 3e).

SNRPB knockdown impacts the expression and processing of RNA splicing machinery components

To assess the contribution of *SNRPB* to GBM development, we performed its knockdown (Additional file 2: Figure S8) followed by RNA-Seq analysis in U251 cells. We then mapped changes in transcriptomic profiles and splicing events compared to control samples.

Table 1 Summary of functional assays results

#	Ensemble ID	Gene symbol	Viability (MTS)		Proliferation (IncuCyte)		Apoptosis (Caspase-3/7)	
			U251	U343	U251	U343	U251	U343
1	ENSG00000106305	*AIMP2*	✓	✓	-	-	-	-
2	ENSG00000183684	*ALYREF*	-	-	-	-	✓	-
3	ENSG00000179218	*CALR*	-	-	-	-	-	-
4	ENSG00000174371	*EXO1*	-	-	-	-	-	-
5	ENSG00000172183	*ISG20*	-	-	✓	-	-	-
6	ENSG00000162385	*MAGOH*	-	-	-	-	✓	-
7	ENSG00000111196	*MAGOHB*	-	-	-	-	✓	-
8	ENSG00000128626	*MRPS12*	-	-	-	-	-	-
9	ENSG00000090263	*MRPS33*	-	✓	-	✓	✓	-
10	ENSG00000132603	*NIP7*	✓	-	✓	✓	-	-
11	ENSG00000132661	*NXT1*	-	✓	✓	-	✓	-
12	ENSG00000111331	*OAS3*	-	-	-	-	-	-
13	ENSG00000171960	*PPIH*	-	-	-	-	-	-
14	ENSG00000153250	*RBMS1*	✓	✓	✓	✓	-	-
15	ENSG00000104889	*RNASEH2A*	✓	✓	✓	✓	✓	-
16	ENSG00000026297	*RNASET2*	-	-	-	-	-	-
17	ENSG00000175792	*RUVBL1*	✓	-	✓	-	✓	-
18	ENSG00000125835	*SNRPB*	✓	✓	✓	✓	✓	✓
19	ENSG00000143977	*SNRPG*	-	-	✓	-	✓	-
20	ENSG00000060138	*YBX3*	-	-	-	-	✓	-
21	ENSG00000088930	*XRN2*	-	✓	✓	-	-	-

✓ = significant difference compared to control (p-value < 0.05)
- = no significant difference compared to control (p-value ≥ 0.05)

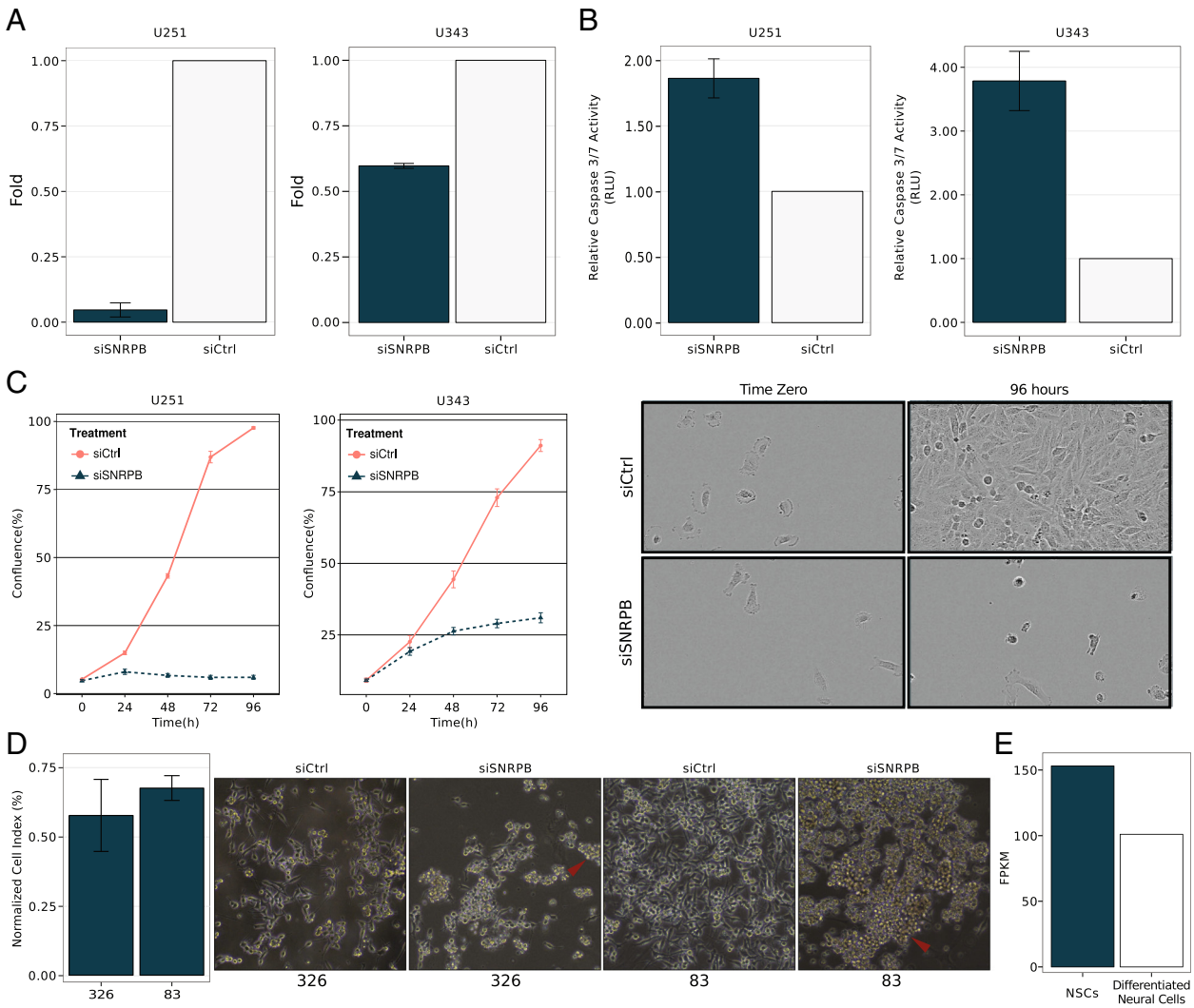

Fig. 3 *SNRPB* impacts cancer-relevant processes. **a** Cellular viability was assayed by MTS and shows that *SNRPB* knockdown caused a significant reduction of viability in U251 (p-value = 0.002; Wilcoxon rank-sum test) and U343 cells (p-value < 0.001; Wilcoxon rank-sum test), compared to control transfected cell lines (*siCtrl*). **b** Caspase-3/7 assay shows an increase in apoptosis in siSNRPB compared to siCtrl in both cell lines (U251 p-value = 0.011; U343 p-value = 0.007; Wilcoxon rank-sum test). **c** Plots show confluence percentage monitored by IncuCyte over 96 hours, comparing siSNRPB with siCtrl. Proliferation reduction was observed in both cell lines upon *SNRPB* knockdown (U251 p-value < 0.001; U343 p-value < 0.001; ANOVA). *Right* panel shows U251 cellular profile at time zero and after 96 hours of transfection with siCtrl and siSNRPB. *SNRPB* knockdown resulted in a strong reduction in cell proliferation compared to control. **d** Downregulation of *SNRPB* by siRNA leads to inhibition of cell growth and cell detachment in two glioma stem cell lines. The percentage of the normalized cell index was calculated with respect to control. Results represent an average of two (line 326) or three (line 83) [39] individual experiments and each experiment was done in triplicate. *Red arrowheads* indicate the floated round up cell colonies on the plates where *SNRPB* siRNA was transfected. **e** *SNRPB* expression in mouse neural stem cells (*NSCs*) was compared to differentiated neural cells after 4 days by RNA-Seq. *SNRPB* expression was higher in undifferentiated cells ($\log_2$ fold change = 0.599347, FDR-adjusted p-value < 0.05)

At the expression level, we found 7118 differentially expressed genes ($\log_2$ fold change > |1| and Benjamini-Hochberg corrected p-value < 0.05) upon *SNRPB* knockdown (3171 upregulated and 3947 downregulated genes; Additional file 1: Table S7). Among the upregulated genes, we observed strong enrichment for biological processes related to RNA processing and metabolism, splicing, and several cellular processes like differentiation, development, proliferation, migration, and signal transduction (Additional file 2: Figure S9A; Additional file 1: Table S8). Downregulated genes were enriched for processes related to DNA repair, DNA metabolism and replication (Additional file 2: Figure S9B; Additional file 1: Table S8).

At the splicing level, we found that 18,105 splicing events were altered upon *SNRPB* knockdown (difference

in percentage spliced in (ΔPSI) > |0.1| and FDR-adjusted p-value < 0.05), affecting a total of 5692 genes. Events were classified in five categories: exon skipping (SE), mutually exclusive exons (MXE), alternative 5′ splice site (A5SS), alternative 3′ splice site (A3SS), or intron retention (RI). A summary showing results classified by event type is presented in Additional file 1: Table S9.

Similar to what was observed in the transcriptomic analysis, we determined that genes affected at the splicing level by *SNRPB* knockdown are preferentially associated with biological processes such as RNA processing and metabolism, splicing, DNA metabolism, and DNA repair (Fig. 4; Additional file 1: Table S10). Additional cancer relevant processes like chromatin remodeling were also identified (Fig. 4; Additional file 1: Table S10). In the particular case of RNA processing and splicing, we determined that core members of the small nuclear ribonucleic proteins (snRNPs), U1, U2, U4/U6, and U5, were greatly affected by *SNRPB* knockdown, especially at the splicing level: almost 60 % of them exhibited splicing alterations, which represents a strong enrichment when this gene set is compared to all multi-exon genes presenting at least one read on exon-exon junctions (p-value = 5.521199e-13; hypergeometric test; Fig. 5). These results suggest that SNRPB coordinates the splicing of spliceosome components.

SNRPB knockdown impacts expression and processing of cancer genes and pathways already associated with gliomagenesis

We also evaluated a set of 368 well-established cancer genes, manually curated from three different large-scale studies [49–51]. Out of 368 genes, 94 presented differential expression (57 upregulated and 37 downregulated). At the splicing level, ~50 % of the cancer genes presented at least one alteration. Enrichment for alterations at expression and splicing levels in this gene set were observed when compared to all expressed genes analyzed and all multi-exon genes presenting at least one read on exon-exon junctions, respectively (expression: p-value = 0.04123; splicing: p-value = 6.45815e-52; hypergeometric test; Fig. 6a, b).

We then specifically checked for alterations in genes involved in critical GBM pathways defined by TCGA: *RTK*, *PI3K*, *RAS*, *MAPK*, *AKT*, *RB*, and *p53* [6, 7]. All pathways were affected by *SNRPB* knockdown. At the expression level, 8 out of 33 evaluated genes were differentially expressed: four of them were upregulated (*HRAS*, *MET*, *NF1*, and *TP53*) and four downregulated upon knockdown (*AKT1*, *AKT2*, *FGFR3*, *PDGFRA*). No enrichment was observed when this category of genes was compared to all expressed genes exhibiting differential expression (p-value = 0.4250002; hypergeometric test). At the splicing level, 18 out of those 33 genes presented at least one differentially

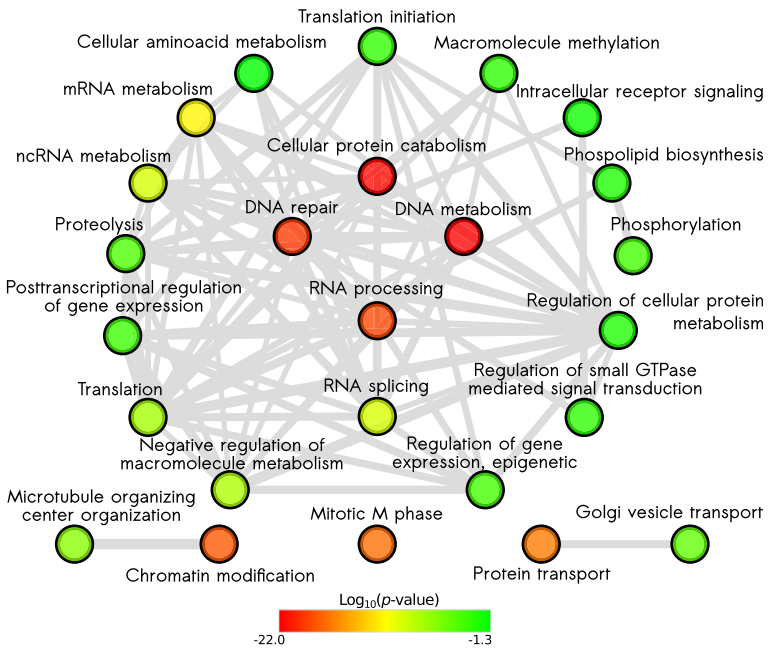

Fig. 4 Gene Ontology (*GO*) annotation of genes presenting splicing alterations upon *SNRPB* knockdown. Network shows interaction between GO terms. *Colors* represent node significance. Top enriched terms were related to RNA processing, DNA metabolism and repair, chromatin modification, and cellular protein catabolism

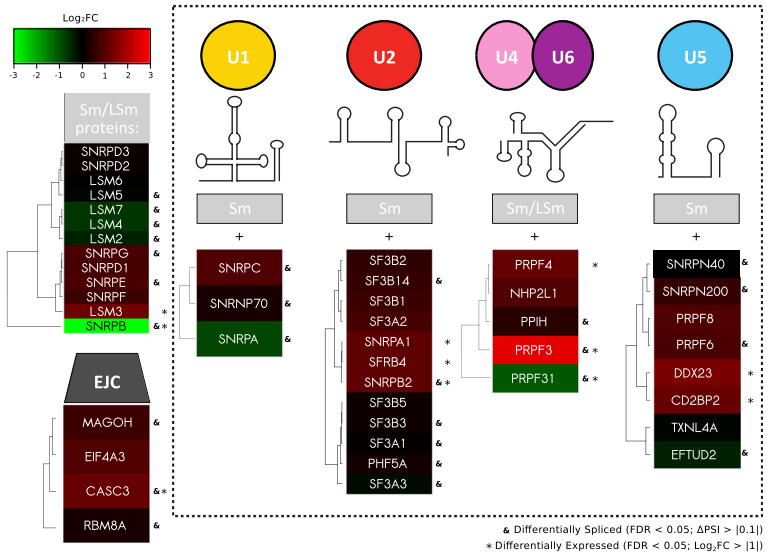

Fig. 5 *SNRPB* knockdown impacts core spliceosome components. More than 20 % of the core spliceosome components were differentially expressed upon *SNRPB* knockdown; meanwhile, almost 60 % of them presented splicing alterations. *EJC* exon-junction complex, *ΔPSI* percentage spliced in. Adapted from [78, 114]

regulated splicing event (Additional file 2: Figure S10), showing strong enrichment for splicing alterations in this specific gene set when compared to all multi-exon genes having at least one read on exon-exon junctions (p-value = 5.409015e-07; hypergeometric test).

Characteristics of exons/introns affected by *SNRPB* knockdown

SE and RI were two of the categories with the highest number of differentially regulated events and therefore were further investigated.

Knockdown of *SNRPB* reduced the inclusion levels of several exons (12,030 events with exons more included in control samples versus 462 events with exons more included in knockdown; Additional file 1: Table S8). Exons with higher exclusion levels upon knockdown were shorter than the ones with higher exclusion levels in control (median knockdown = 106 nucleotides, median control = 148 nucleotides; p-value < 2.2e-16; Wilcoxon-rank sum test; Additional file 2: Figure S11 left panel). With respect to GC content, exons whose inclusion in mature transcripts decreased upon *SNRPB* knockdown exhibited a lower percentage of GC when compared to the ones showing the opposite behavior (median knockdown = 47.25 %; median control = 50.57 %; p-value = 5.936e-07; Wilcoxon rank-sum test; Additional file 2: Figure S12 left panel). We also examined the strength of 3′ and 5′ splice sites (3′ss and 5′ss) associated with exons affected by *SNRPB* knockdown using the MaxEntScan approach [52]. Exons with higher exclusion levels upon knockdown were associated with stronger 3′ss and 5′ss compared to control (3′ss p-value < 2.2e-16; 5′ss p-value = 2.092e-14; Wilcoxon rank-sum test; Additional file 2: Figure S13 top panel).

Regarding introns, we observed that *SNRPB* knockdown favored the retention of introns in mature transcripts (835 intron retention events in knockdown compared to 116 in control samples; Additional file 1: Table S8). Introns showing increased retention in mature transcripts upon *SNRPB* knockdown were determined to be shorter than the ones preferentially retained in control samples (median knockdown = 483 nucleotides; median control = 1144 nucleotides; p-value < 2.2e-16; Wilcoxon rank-sum test; Additional file 2: Figure S11 right panel). Considering the GC content, introns more retained upon *SNRPB* knockdown presented a higher percentage of GC compared to the ones more retained in control (median knockdown = 59.07 %; median control = 43.96 %; p-value < 2.2e-16; Wilcoxon rank-sum test; Additional file 2: Figure S12 right panel). No significant difference was observed in the strength of 5′ss 3′ss associated with differentially regulated introns (3′ss p-value = 0.4464; 5′ss p-value = 0.9095; Wilcoxon rank-sum test; Additional file 2: Figure S13 bottom panel).

We also determined the effect of *SNRPB* knockdown on “constitutive” versus “alternative” exons and introns. Constitutive exons and introns were defined as those presenting with a PSI value = 1 and PSI = 0 in the control samples, respectively, whereas alternative exons and introns were defined as those with a PSI value < 1 (for exons) and PSI value > 0 (for introns) in control samples. In total, 5.6 % of the constitutive exons were affected by *SNRPB* knockdown, while 20.1 % of alternative

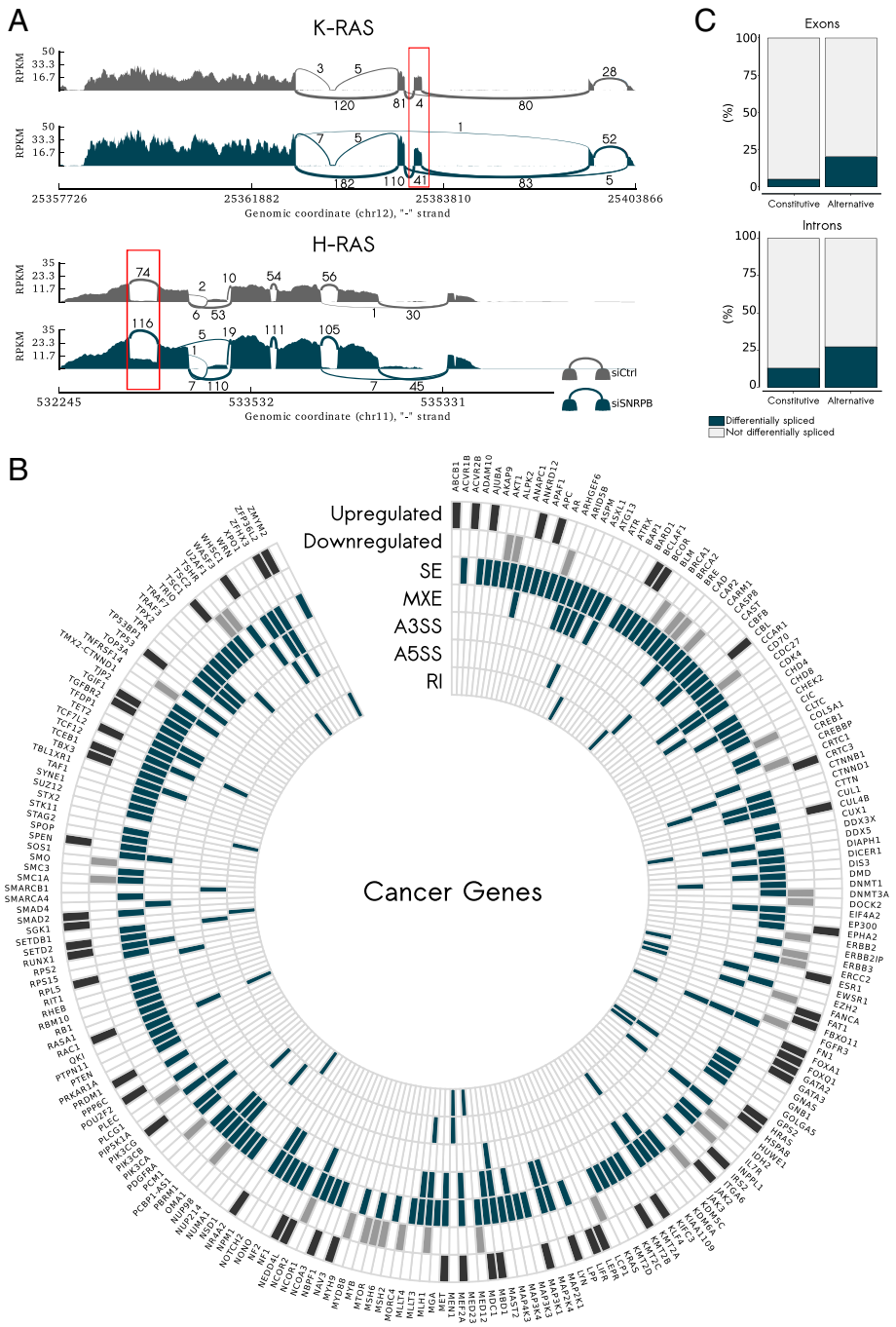

Fig. 6 SNRPB impact on cancer genes and on alternative/constitutive exons/introns. **a** Sashimi plots highlighting two splicing events differentially regulated in siSNRPB compared with siCtrl: an exon skipping event in K-RAS (*top panel*) and an intron retention in H-RAS (*bottom panel*). **b** A total of 368 cancer genes were evaluated. Only genes presenting differential expression (upregulated or downregulated) or at least one splicing alteration [exon skipping (*SE*), mutually exclusive exons (*MXE*), alternative 5′ splice site (*A5SS*), alternative 3′ splice site (*A3SS*), or intron retention (*RI*)] are shown. **c** Alternative exons and introns are more affected by *SNRPB* knockdown than constitutive exons and introns

exons showed changes (p-value < 2.2e-16; proportion test; Fig. 6c top panel). Regarding introns, 12.5 % of the constitutive ones were affected, while 26.4 % of the alternative introns presented alterations (p-value < 2.2e-16; proportion test; Fig. 6c bottom panel).

In summary, exons with higher exclusion levels upon *SNRPB* knockdown were shorter, and had lower GC content, and stronger 3′ss and 5′ss, whereas introns with higher retention levels upon knockdown were shorter, and exhibited higher GC content and no difference in 3′ss and

5′ss strength compared to the ones more retained in control samples.

Discussion

Major changes in the expression of RBP coding genes are a noteworthy phenomena in multiple tumor tissues [16–18]. Here, we have corroborated this scenario in GBM. By comparing tumor samples (GBM samples from TCGA and GSC lines) to normal samples, we identified a set of 21 upregulated RBPs that also exhibited an impact on patient survival. We also found the expression levels of those RBPs was higher in GBMs than in lower grade gliomas, suggesting their potential impact on tumor progression and aggressiveness. To explore mechanisms that could contribute to the upregulation of those RBPs, we analyzed non-synonymous mutations, CNAs, and targeting by tumor suppressor miRNAs. We observed a modest contribution of mutations and CNAs. Because GBM does not exhibit a high mutational load compared to other tumor types [53], and has only 71 genes that are frequently mutated [7], the low number of samples harboring mutations in a small set of RBPs was expected. Regarding the tumor suppressor miRNAs, we found 18 of them targeting 15 out of 21 RBPs. Notably, miR-124 alone targets six RBPs. miR-124 is an important player in GBMs and impacts proliferation [54], tumor growth [55, 56], migration, and invasion [57].

The impact of RBP alterations in cancer is still poorly appreciated. One of the main reasons is that most available datasets include only mRNA expression levels, preventing any type of analysis to measure changes in splicing, mRNA decay, and translation. However, this scenario is improving, especially with the advent of functional genomics methods, like ribosomal profiling and more sensitive proteomics platforms. In addition, the transcriptomics field is moving away from microarray towards RNA-Seq, which provides an opportunity to investigate global changes in splicing [58]. Recent investigations of alternative splicing across multiple cancer types have revealed splicing as an important source of transcriptional diversity in many cancers and allowed the identification of a common set of cancer-specific splicing events, which can potentially be used as novel biomarkers with application in molecular diagnosis and prognosis [59–61].

We identified an interesting subset of aberrantly expressed RBPs implicated in splicing, pointing to an additional layer of alterations that could contribute to GBM development. Involvement of splicing proteins in cancer and other disorders is capturing the interest of the scientific community. One of the most studied cases is *SF3B1*, which is mutated in ~20 % of patients with myelodysplastic syndromes (MDS). Other splicing regulators, including *PRPF40B*, *SRSF2*, *SF3A1*, *U2AF1*, and *ZRSR2*, also display a high mutation frequency in MDS [62]. Studies of hematological malignancies showed similar results. For instance, *SF3B1*, *SRSF1*, *U2AF65*, and *CELF4* are often mutated in chronic lymphocytic leukemia [63]. Subsequent reports revealed that alterations in splicing factors occur in solid tumors, including neuroblastomas, pancreatic ductal adenocarcinoma, lung cancer, melanoma, colon cancer, and estrogen receptor-positive breast tumors [64, 65]. In GBM, the splicing factors PTB, hnRNP H and A2/B1, and WTAP have been shown to regulate several biological processes relevant to cancer development [29–34, 66]. Moreover, numerous examples of cancer-relevant genes affected at the splicing level (e.g. *ANXA7*, *GLI1*, *MAX*, *KLF6*) have been reported in GBM [30, 31, 34, 67–70]. Besides contributing to tumorigenesis via splicing regulation, splicing factors can have additional routes of action. For instance, genomic instability, a common feature in cancer, can be induced by RNA processing defects [71].

SNRPB, which encodes core members of the spliceosome machinery, SmB/B′, was the main focus of our study. Its knockdown decreased viability, increased apoptosis, and decreased proliferation in both U251 and U343 cell lines. One would expect that alterations in core splicing proteins, such as the ones encoded by *SNRPB*, could cause major disruptions in RNA processing, affecting the entire transcriptome in a global and homogeneous manner. However, a different scenario has been observed, with splicing regulators impacting distinct sets of events when their expression levels are altered. For instance, in a recent study, 270 core splicing proteins and other RNA-related factors were systematically knocked down and the impact on splicing of 38 genes associated with proliferation and apoptosis was investigated [72]. It was observed that each splicing factor regulated a specific set of events, and factors involved in the same splicing step tended to affect the same group of events. Results were corroborated by RNA-Seq studies in which specific changes in splicing, mainly in alternative exons, were observed upon knockdown of core splicing proteins, including SNRPB [73–75].

In addition to its essential role in splicing, mutations in *SNRPB* are known to cause cerebro-costo-mandibular syndrome [76–78]. Furthermore, a screening for genes required for cell division revealed *SNRPB* along with other splicing factors [79]. However, *SNRPB* is relatively poorly characterized in terms of contributions to tumorigenesis. Its expression is altered in non-small cell lung cancer along with other genes involved in RNA metabolism and is correlated with a poor prognosis [80]. In a mouse allograft model of prostate cancer (NE-10), *SNRPB* was identified as a candidate metastasis suppressor gene [81]. Quantitative expression analysis confirmed decreased expression of SNRPB in the metastasizing

compared to non-metastasizing tumors [81]. These data along with ours suggest that SNRPB can have different roles in tumorigenesis depending on context.

Alternative splicing events can result in transcript isoforms with reading frame disruption, lower stability, and improper localization in comparison to constitutive isoforms. Our RNA-Seq analysis determined some trends in terms of splicing events upon *SNRPB* knockdown. Alternative exons and introns were more affected than the constitutive ones, suggesting SNRPB functions to help the recognition of exons and introns containing weaker regulatory elements, such as alternative exons.

Gene ontology enrichment analysis of gene expression and splicing data revealed that *SNRPB* influences a large number of biological processes with relevance to cancer, such as RNA processing and DNA repair. Alterations in a large number of RNA processing/splicing genes places *SNRPB* as a central regulator and suggests that several of the splicing alterations we observed upon *SNRPB* knockdown might be in fact a secondary effect. Radioresistance, which is largely influenced by genes in the DNA repair pathway, is a major problem in cancer treatment and it is particularly relevant to GBM. Splicing alterations have been described for a large number of DNA repair genes, including several that we determined to be influenced by SNRPB levels (*BRAC1*, *BARD1*, *MSH2*, *RAD50*, *CHEK1*) [82–86]. Additionally, we observed that knockdown of *SNRPB* altered multiple genes associated with critical genes/pathways relevant to GBM development (*RTK*, *PI3K*, *MAPK*, *RAS*, *AKT*, *RB*, and *p53*) and other cancer genes.

Conclusion

Despite the need for a more detailed analysis to determine how alterations identified here affect protein function in specific ways to contribute to tumor initiation and growth, we conclude that our data suggest diverse routes by which SNRPB influences GBM development.

Methods

Gene expression analysis of GBM RNA-Seq data from TCGA

RNA-Seq raw reads from 170 samples of GBM from TCGA [87] were downloaded from Cancer Genomics Hub (CGHub [88]; Additional file 1: Table S1). Normal brain samples were downloaded from the SRA [89] database [SRA: SRP028705 and ERP003613], Human Body Map [SRA: ERR030882], and TCGA (Additional file 1: Table S1). Reads were mapped against the human genome (version hg19/GRCh37 – UCSC Genome Browser [90]) using GSNAP [91] (version 2014-05-15). Mapped reads with quality (Q) ≥ 20 (Phred scale) were selected using SAMtools [92]. Read counts per gene were defined using HTSeq [93] and GENCODE (version 19 [15]) as the reference transcriptome. Differential expression analysis was performed using DESeq2 [94] comparing tumor samples to normal samples. All genes differentially expressed between tumor and normal samples (Benjamini-Hochberg corrected p-value < 0.05 and $\log_2$ fold change ≥ |1|) were selected. The catalog containing 1542 human RBPs from Gerstberger et al. [14] was used as a reference to identify all differentially expressed RBPs.

Gene expression analysis of GSCs microarray data

Microarray data (Affymetrix platform: Human U219) of 10 glioma stem cell lines and one normal neural progenitor cell line, in triplicate, were obtained from Mao et al. [39]. Data were normalized using Robust Multichip Average (RMA; Affy package [95]). Differentially expressed RBPs between normal and GSC samples (Benjamini-Hochberg corrected p-value < 0.05) were identified using the LIMMA package [96].

Survival analysis

The REMBRANDT dataset (REpository for Molecular BRAin Neoplasia DaTa [42]) was used to evaluate whether increased expression of the selected RBPs was associated with a poorer prognosis in brain neoplasia. Samples with increased expression of selected RBPs ($\log_2$ fold change ≥ 1) were compared to all other samples. Kaplan-Meier survival curves were built and then compared using a log-rank test. Differences resulting in a p-value < 0.05 were considered significant.

Comparison of normal brain samples from GTEx with GBM samples from TCGA

Read counts per gene of 222 samples from normal brain (cortex and frontal cortex) were downloaded from the GTEx portal [43]. Those samples were compared to 170 GBM samples from TCGA. Read counts per gene of GBM samples were generated as described previously. Differential expression analysis was performed using DESeq2 [94], comparing tumor to normal samples, and the expression levels of 21 RBPs were analyzed. RBPs presenting Benjamini-Hochberg corrected p-values < 0.05 were considered to be differentially expressed.

RBPs expression in lower and higher grade gliomas

Level 3 normalized expression data from 167 grade IV gliomas (GBMs) and 218 lower grade gliomas (LGG: 31 grade II astrocytomas, 73 grade II oligodendrogliomas, 68 grade III astrocytomas, and 46 grade III oligodendrogliomas) were downloaded from TCGA [87]. Expression levels of 21 RBPs in LGG were compared with GBM samples using Wilcoxon rank-sum test.

Mutation and CNA analysis

All 273 GBM samples with exome sequencing and CNA data available in cBioPortal [45, 46] were evaluated (dataset: Glioblastoma Multiforme – TCGA, Provisional). The gene set containing 21 selected RBPs was analyzed and all samples containing at least one alteration in one or more of these RBPs were identified and presented. A simulation with 100,000 random sets of 21 out of 1542 RBPs was performed to determine if our selected set presented enrichment for CNA and mutations. Mutation and CNA data for all RBPs were retrieved from cBioPortal using the CDGS-R package [97].

Tumor suppressor miRNAs targeting RBPs

A list containing frequently downregulated miRNAs in GBM (tumor suppressor miRNAs) was downloaded from Hermansen and Kristensen [44]. We then used the miRTarBase database [98] to select all genes targeted by those tumor suppressor miRNAs. Next, we identified which of those miRNAs target at least one of the 21 selected RBPs. Enrichment was calculated using a hypergeometric test.

Functional annotation

Functional annotation analyses (Gene Ontology and KEGG pathways) were performed using DAVID [99], using *Homo sapiens* genes as background. Terms with Benjamini-Hochberg corrected p-values < 0.05 were determined as enriched. Redundant GO terms were summarized using REViGO [100]. Networks of GO terms were built using Cytoscape [101].

Cell growth and transfection

U251 and U343 GBM cells (from American Type Culture Collection, Manassas, VA, USA) were grown in Dulbecco's Modified Eagle medium with 10 % fetal bovine serum. Cells were synchronized through serum starvation for 48 hours. siRNAs (ON-TARGETplus SMARTpool; Dharmacon) for 21 RBPs and one siRNA control were transfected using Lipofectamine RNAiMax reagent (Invitrogen) according to the manufacturer's instructions. All following experiments were performed in triplicate.

We established serum-free 3D cultures from two individual GSC lines (326 and 83) previously obtained by Dr Ichiro Nakano [39] during his time at The Ohio State University. Information regarding the Human Protocol and patient consent are described in the original publication [39]. Cells were trypsinized using TrypLE (Invitrogen) and plated in a collagen-coated T-25 flask with 10,000 irradiated (3000 rad) human mesenchymal stem cells (Lonza) in a conditionally reprogrammed FY medium [3:1 (v/v) F-12 Nutrient Mixture (Ham)/Dulbecco's Modified Eagle medium (Invitrogen), 5 % fetal bovine serum, 0.4 μg/mL hydrocortisone (Sigma-Aldrich), 5 μg/mL insulin (Sigma-Aldrich), 8.4 ng/mL cholera toxin (Sigma-Aldrich), and 10 ng/mL epidermal growth factor (Invitrogen)] with the addition of 5 μmol/L Y-27632 (Enzo Life Sciences) [47]. Cells were grown in a humidified incubator at 37 °C with 5 % carbon dioxide for several passages to ensure the stability of cultures. For knockdown experiments, 200,000 GSC cells were plated in a collagen-coated six-well plate along with 2000 irradiated human mesenchymal stem cells in conditionally reprogrammed cell media containing FY medium. The next day, 25 nM of either scrambled or *SNRPB* siRNA suspended in RNAiMAX was added to the wells. Subsequently, each well was washed twice with phosphate-buffered saline and 500 μL of OPTIMEM was added. After 5–6 hours, 2 mL of conditionally reprogrammed media was incorporated into each well. After 72 hours, the floating cell fraction was collected and mixed with trypsinized attached cells from each well. Cell counting was performed using a Countess automated cell counter (Life Technologies) according to the manufacturer's protocol. Transfections were performed in triplicate and each experiment was done at least two times. Total RNA was isolated by pooling three wells from each experiment and using an RNeasy kit (Qiagen) according to the manufacturer's instructions. The percentage normalized cell index for SNRPB-specific siRNA was calculated by normalizing the cell index with control siRNA. The standard deviation was calculated for each experiment and then averaged to obtain cumulative standard deviation.

Cell viability assay

After transfection, U251 and U343 cells were grown in 96-well cell culture plates. Cell viability was assessed by CellTiter 96 AQueous One Solution (Promega) reagent after 72 hours of incubation. Absorbance at 490 nm was quantified using the SpectraMax M5 microplate reader (Molecular Devices). Data were analyzed using Student's t-test and presented as the relative mean ± standard error.

Proliferation assay

After transfection, U251 and U343 cells were grown in 96-well cell culture plates. The confluence percentage was monitored for 96 hours using a high-definition automated imaging system (IncuCyte; Essen BioScience). Data were evaluated using ANOVA and presented as mean ± standard error.

Caspase-3/7 apoptosis assay

U251 and U343 cells were grown in 96-well plates after transfection. After 72 hours of incubation, apoptosis levels were assessed using the Caspase-Glo 3/7 assay

kit (Promega), according to the manufacturer's protocol. Luminescence was measured using the SpectraMax M5 microplate reader (Molecular Devices). Data were analyzed using Student's *t*-test and presented as mean of relative light units ± standard error.

Gene expression analysis of RNA-Seq data from neural stem cells

RNA-Seq data from mouse neural stem cells and differentiated cells after 4 days [GEO: GSE67135] was used to analyze expression levels of *SNRPB* in both conditions. The HomoloGene database [102] was used to identify *SNRPB* orthologs between human and mouse. *SNRPB* gene expression in undifferentiated cells was compared to its expression in differentiated neural cells.

Knockdown quantification by real-time PCR

Total RNA was extracted using TRIzol reagent (Invitrogen) according to manufacturer's instructions. Reverse transcription of messenger RNAs was performed using a high-capacity cDNA reverse transcription kit (Applied Biosystems) with random priming. For mRNA analysis, quantitative PCR was performed using the primers listed in Additional file 1: Table S6 and Power SYBR Green PCR Master Mix (Applied Biosystems). Real-time PCRs were performed on the ViiA™ 7 Real-Time PCR System (Applied Biosystems). Data were acquired using the ViiA 7 RUO software (Applied Biosystems) and analyzed using the $2^{-\Delta\Delta CT}$ method with GAPDH as an endogenous control.

Knockdown quantification by western blot

Cells were resuspended and sonicated in Laemmli sample buffer, separated on a 13.5 % sodium dodecyl sulfate polyacrylamide gel electrophoresis (SDS-PAGE) gel, and transferred to polyvinylidene fluoride (PVDF) membranes. After transfer, membranes were blocked in Tris-buffered saline with Tween 20 and 5 % milk. Membranes were probed with rabbit anti-α-SNRPB (GeneTex; dilution 1:500) and mouse anti-α-tubulin antibody (Sigma; dilution, 1:2000). Horseradish peroxidase (HRP)-conjugated goat anti-rabbit antibody (Santa Cruz Biotechnology) or HRP-conjugated goat anti-mouse antibody (Zymed Laboratories, Carlsbad, CA, USA) were used as secondary antibodies. Electrochemiluminescence was used to detect the selected proteins using Immobilon Western chemiluminescent substrate (Millipore, Billerica, MA, USA).

RNA preparation and sequencing

U251 cells were transiently transfected with control or SNRPB siRNAs using Lipofectamine RNAiMAX (Invitrogen). The experiment was performed in triplicate. Knockdown levels of SNRPB were ~90 %, as measured by quantitative reverse transcription-PCR (qRT-PCR). Total RNA was extracted using the TRIzol reagent (Life Technologies) and further purified with RNeasy (Qiagen), according to manufacturer's instructions. Samples were prepared for RNA-Seq according to Illumina instructions and sequenced in a HiSeq-2000 machine by UTHSCSA Genomic Facility.

Alternative splicing analysis

To identify splicing alterations produced by *SNRPB* knockdown, raw RNA-Seq reads of control and knockdown experiments were mapped against the human reference genome (hg19/GRCh37) and a reference transcriptome (GENCODE version 19 [15]) using GSNAP [91] (version 2014-05-15). Next, only reliable alignments ($Q \geq 20$; Phred-scale) were selected using SAMtools [92]. Multivariate Analysis of Transcript Splicing (MATS [103, 104]) was used to search for splicing differences between *SNRPB*-knockdown and control samples. Only those isoforms differentially represented between conditions (FDR-adjusted p-value < 0.05 and $\Delta PSI > |0.1|$) were selected. Splicing variants were classified as SE, MXE, RI, alternative donor site (A5SS), or alternative acceptor site (A3SS). 3′ss and 5′ss strengths of the differentially spliced exons and introns were calculated using the MaxEntScan approach [52].

Statistical analysis and figures

All statistical analyses were executed using R [105]. Figures were built using R [105], Cytoscape [101], Circos Plot [106], Sashimi plot [107], and Inkscape [108].

Additional files

Additional file 1: Contains supplementary **Tables S1–S10. Table S1.** GBM RNA-Seq samples from TCGA and Normal samples from SRA and TCGA. **Table S2.** Differentially expressed RBPs in GBM data from TCGA. **Table S3.** Differentially expressed RBPs in GSCs data. **Table S4.** RBPs expression in GBM samples from TCGA vs. normal brain samples from GTEx. **Table S5.** Wilcoxon rank-sum test results: GBM vs. lower grade gliomas. **Table S6.** Knockdown efficiency measured by qRT-PCR. **Table S7.** Differentially expressed genes upon *SNRPB* knockdown. **Table S8.** Functional annotation of differentially expressed genes upon *SNRPB* knockdown. **Table S9.** Summary of differentially regulated splicing events upon *SNRPB* knockdown. **Table S10.** Functional annotation of differentially spliced genes upon *SNRPB* knockdown. (XLS 822 kb)

Additional file 2: Contains supplementary **Figures S1–S13.** (PDF 4857 kb)

Acknowledgements

We would like to thank Dr Ichiro Nakano for sharing cell lines and Dr Scott Kuersten for comments. The results published here are in part based upon data generated by TCGA Research Network: http://cancergenome.nih.gov/.

Funding

This study was supported by a grant from the Conselho Nacional de Desenvolvimento Científico e Tecnológico (CNPq), Brazil, to PFG and LOFP and 5R21CA205475-02 to LOFP. BRC was supported by fellowships from Fundação de Amparo a Pesquisa do Estado de São Paulo – FAPESP (2013/25483-4 and 2013/07159-5). PRA was supported by CPRIT Training Grant RP140105.

Availability of data and materials
RNA sequencing data have been deposited in the European Nucleotide Archive [ENA: PRJEB10298] [109].

Authors' contributions
BRC performed all the computational and statistical analyses, helped with experiments, and wrote parts of the manuscript. PRA performed qRT-PCR experiments and helped with biological assays. MQ performed the majority of the biological assays. SCB prepared the RNA-Seq library and helped with biological assays. CC established patient-derived cell cultures and performed the knockdown assays on these cell lines. RS helped with the establishment of CRC lines. SA supervised, designed, and analyzed the knockdown experiments in patient-derived cell lines. PAFG designed the study, led computational analysis, and wrote parts of the manuscript. LOFP designed the study, led data interpretation, and wrote parts of the manuscript. All authors read and approved the final manuscript.

Competing interests
The authors declare that they have no competing interests.

Ethics approval and consent to participate
All experimental methods comply with the Helsinki Declaration. GSC lines used in Fig. 3d were obtained by Dr Ichiro Nakano's laboratory (The Ohio State University) and are described in [39]. All work relating to human tissues was performed previously at Ohio State University (Columbus, OH, USA) under an institutional review board–approved protocol according to National Institute of Health (NIH) guidelines. Glioma neurospheres were obtained from high-grade glioma samples using protocols described previously [110–113]. Drs I. Nakano and E. A. Chiocca performed the surgeries at the Department of Neurological Surgery, The Ohio State University (Columbus, OH, USA).

Author details
[1]Centro de Oncologia Molecular, Hospital Sírio-Libanês, São Paulo, Brazil. [2]Children's Cancer Research Institute, UTHSCSA, San Antonio, TX, USA. [3]Georgetown University Medical Center, Washington, DC, USA. [4]Department of Cellular and Structural Biology, UTHSCSA, San Antonio, TX, USA.

Received: 5 February 2016 Accepted: 24 May 2016
Published online: 10 June 2016

References
1. Omuro AMP, Faivre S, Raymond E. Lessons learned in the development of targeted therapy for malignant gliomas. Mol Cancer Ther. 2007;6:1909–19.
2. Stupp R, Mason WP, van den Bent MJ, Weller M, Fisher B, Taphoorn MJB, Belanger K, Brandes AA, Marosi C, Bogdahn U, Curschmann J, Janzer RC, Ludwin SK, Gorlia T, Allgeier A, Lacombe D, Cairncross JG, Eisenhauer E, Mirimanoff RO. Radiotherapy plus concomitant and adjuvant temozolomide for glioblastoma. N Engl J Med. 2005;352:987–96.
3. Holland EC. Glioblastoma multiforme: the terminator. Proc Natl Acad Sci U S A. 2000;97:6242–4.
4. Furnari FB, Fenton T, Bachoo RM, Mukasa A, Stommel JM, Stegh A, Hahn WC, Ligon KL, Louis DN, Brennan C, Chin L, DePinho RA, Cavenee WK. Malignant astrocytic glioma: genetics, biology, and paths to treatment. Genes Dev. 2007;21:2683–710.
5. Esparza R, Azad TD, Feroze AH, Mitra SS, Cheshier SH. Glioblastoma stem cells and stem cell-targeting immunotherapies. J Neurooncol. 2015;123:449–57.
6. McLendon R, Friedman A, Bigner D, Van Meir EG, Brat DJ, Mastrogianakis GM, Olson JJ, Mikkelsen T, Lehman N, Aldape K, Alfred Yung WK, Bogler O, VandenBerg S, Berger M, Prados M, Muzny D, Morgan M, Scherer S, Sabo A, Nazareth L, Lewis L, Hall O, Zhu Y, Ren Y, Alvi O, Yao J, Hawes A, Jhangiani S, Fowler G, San Lucas A, et al. Comprehensive genomic characterization defines human glioblastoma genes and core pathways. Nature. 2008;455:1061–8.
7. Brennan CW, Verhaak RGW, McKenna A, Campos B, Noushmehr H, Salama SR, Zheng S, Chakravarty D, Sanborn JZ, Berman SH, Beroukhim R, Bernard B, Wu C-J, Genovese G, Shmulevich I, Barnholtz-Sloan J, Zou L, Vegesna R, Shukla SA, Ciriello G, Yung WK, Zhang W, Sougnez C, Mikkelsen T, Aldape K, Bigner DD, Van Meir EG, Prados M, Sloan A, Black KL, et al. The somatic genomic landscape of glioblastoma. Cell. 2013;155:462–77.
8. Bonavia R, Inda MDM, Cavenee WK, Furnari FB. Heterogeneity maintenance in glioblastoma: a social network. Cancer Res. 2011;71:4055–60.
9. Persano L, Rampazzo E, Basso G, Viola G. Glioblastoma cancer stem cells: role of the microenvironment and therapeutic targeting. Biochem Pharmacol. 2013;85:612–22.
10. Friedmann-Morvinski D. Glioblastoma heterogeneity and cancer cell plasticity. Crit Rev Oncog. 2014;19:327–36.
11. Castello A, Fischer B, Eichelbaum K, Horos R, Beckmann BM, Strein C, Davey NE, Humphreys DT, Preiss T, Steinmetz LM, Krijgsveld J, Hentze MW. Insights into RNA biology from an atlas of mammalian mRNA-binding proteins. Cell. 2012;149:1393–406.
12. Castello A, Horos R, Strein C, Fischer B, Eichelbaum K, Steinmetz LM, Krijgsveld J, Hentze MW. System-wide identification of RNA-binding proteins by interactome capture. Nat Protoc. 2013;8:491–500.
13. Klass DM, Scheibe M, Butter F, Hogan GJ, Mann M, Brown PO. Quantitative proteomic analysis reveals concurrent RNA-protein interactions and identifies new RNA-binding proteins in Saccharomyces cerevisiae. Genome Res. 2013;23:1028–38.
14. Gerstberger S, Hafner M, Tuschl T. A census of human RNA-binding proteins. Nat Rev Genet. 2014;15:829–45.
15. GENCODE Project. [http://www.gencodegenes.org/].
16. Galante PAF, Sandhu D, Abreu RDS, Gradassi M, Vogel C, De Souza SJ, Penalva LOF. A comprehensive in silico expression analysis of RNA binding proteins in normal and tumor tissue: identification of potential players in tumor formation. RNA Biol. 2009;6:426–33.
17. Kechavarzi B, Janga SC. Dissecting the expression landscape of RNA-binding proteins in human cancers. Genome Biol. 2014;15:R14.
18. Wang J, Liu Q, Shyr Y. Dysregulated transcription across diverse cancer types reveals the importance of RNA-binding protein in carcinogenesis. BMC Genomics. 2015;16 Suppl 7:S5.
19. Abdelmohsen K, Gorospe M. Posttranscriptional regulation of cancer traits by HuR. Wiley Interdiscip Rev RNA. 2010;1:214–29.
20. Glazer RI, Vo DT, Penalva LOF. Musashi1: an RBP with versatile functions in normal and cancer stem cells. Front Biol (Beijing). 2012;17:54–64.
21. Bielli P, Busà R, Paronetto MP, Sette C. The RNA-binding protein Sam68 is a multifunctional player in human cancer. Endocr Relat Cancer. 2011;18:R91–R102.
22. Jia Y, Polunovsky V, Bitterman PB, Wagner CR. Cap-dependent translation initiation factor eIF4E: an emerging anticancer drug target. Med Res Rev. 2012;32:786–814.
23. Yeo G, Holste D, Kreiman G, Burge CB. Variation in alternative splicing across human tissues. Genome Biol. 2004;5:R74.
24. Wang ET, Sandberg R, Luo S, Khrebtukova I, Zhang L, Mayr C, Kingsmore SF, Schroth GP, Burge CB. Alternative isoform regulation in human tissue transcriptomes. Nature. 2008;456:470–6.
25. Castle JC, Zhang C, Shah JK, Kulkarni AV, Kalsotra A, Cooper TA, Johnson JM. Expression of 24,426 human alternative splicing events and predicted cis regulation in 48 tissues and cell lines. Nat Genet. 2008;40:1416–25.
26. Muto J, Imai T, Ogawa D, Nishimoto Y, Okada Y, Mabuchi Y, Kawase T, Iwanami A, Mischel PS, Saya H, Yoshida K, Matsuzaki Y, Okano H. RNA-binding protein Musashi1 modulates glioma cell growth through the post-transcriptional regulation of Notch and PI3 Kinase/Akt signaling pathways. PLoS One. 2012;7:e33431.
27. Vo DT, Abdelmohsen K, Martindale JL, Qiao M, Tominaga K, Burton TL, Gelfond JAL, Brenner AJ, Patel V, Trageser D, Scheffler B, Gorospe M, Penalva LOF. The oncogenic RNA-binding protein Musashi1 is regulated by HuR via mRNA translation and stability in glioblastoma cells. Mol Cancer Res. 2012;10:143–55.
28. Uren PJ, Vo DT, de Araujo PR, Pötschke R, Burns SC, Bahrami-Samani E, Qiao M, de Sousa Abreu R, Nakaya HI, Correa BR, Kühnöl C, Ule J, Martindale JL, Abdelmohsen K, Gorospe M, Smith AD, Penalva LOF. RNA-binding protein Musashi1 is a central regulator of adhesion pathways in glioblastoma. Mol Cell Biol. 2015;35:2965–78.
29. Clower CV, Chatterjee D, Wang Z, Cantley LC, Vander Heiden MG, Krainer AR. The alternative splicing repressors hnRNP A1/A2 and PTB influence pyruvate kinase isoform expression and cell metabolism. Proc Natl Acad Sci U S A. 2010;107:1894–9.
30. LeFave CV, Squatrito M, Vorlova S, Rocco GL, Brennan CW, Holland EC, Pan Y-X, Cartegni L. Splicing factor hnRNPH drives an oncogenic splicing switch in gliomas. EMBO J. 2011;30:4084–97.
31. Golan-Gerstl R, Cohen M, Shilo A, Suh SS, Bakàcs A, Coppola L, Karni R. Splicing factor hnRNP A2/B1 regulates tumor suppressor gene splicing and is an oncogenic driver in glioblastoma. Cancer Res. 2011;71:4464–72.

32. Deng J, Chen S, Wang F, Zhao H, Xie Z, Xu Z, Zhang Q, Liang P, Zhai X, Cheng Y. Effects of hnRNP A2/B1 knockdown on inhibition of glioblastoma cell invasion. Mol Neurobiol. 2016;53:1132–44.
33. Jin W, McCutcheon IE, Fuller GN, Huang ES, Cote GJ. Fibroblast growth factor receptor-1 alpha-exon exclusion and polypyrimidine tract-binding protein in glioblastoma multiforme tumors. Cancer Res. 2000;60:1221–4.
34. McCutcheon IE, Hentschel SJ, Fuller GN, Jin W, Cote CJ. Expression of the splicing regulator polypyrimidine tract-binding protein in normal and neoplastic brain. Neuro Oncol. 2004;6:21–7.
35. Germano IM, Binello E. Stem cells and gliomas: past, present, and future. J Neurooncol. 2014;119:547–55.
36. Bao S, Wu Q, McLendon RE, Hao Y, Shi Q, Hjelmeland AB, Dewhirst MW, Bigner DD, Rich JN. Glioma stem cells promote radioresistance by preferential activation of the DNA damage response. Nature. 2006;444:756–60.
37. Liu G, Yuan X, Zeng Z, Tunici P, Ng H, Abdulkadir IR, Lu L, Irvin D, Black KL, Yu JS. Analysis of gene expression and chemoresistance of CD133+ cancer stem cells in glioblastoma. Mol Cancer. 2006;5:67.
38. Chen J, Li Y, Yu T-S, McKay RM, Burns DK, Kernie SG, Parada LF. A restricted cell population propagates glioblastoma growth after chemotherapy. Nature. 2012;488:522–6.
39. Mao P, Joshi K, Li J, Kim S-H, Li P, Santana-Santos L, Luthra S, Chandran UR, Benos P V, Smith L, Wang M, Hu B, Cheng S-Y, Sobol RW, Nakano I. Mesenchymal glioma stem cells are maintained by activated glycolytic metabolism involving aldehyde dehydrogenase 1A3. Proc Natl Acad Sci U S A. 2013;110:8644–9.
40. Zhao Y, Adjei AA. Targeting oncogenic drivers. Prog Tumor Res. 2014;41:1–14.
41. Mohr SE, Smith JA, Shamu CE, Neumüller RA. RNAi screening comes of age: improved techniques and complementary approaches. Nat Publ Gr. 2014;15:591–600.
42. REMBRANDT: Repository for Molecular Brain Neoplasia Data. [https://caintegrator.nci.nih.gov/rembrandt/]
43. GTEx Portal. [http://www.gtexportal.org/]
44. Hermansen SK, Kristensen BW. MicroRNA biomarkers in glioblastoma. J Neurooncol. 2013;114:13–23.
45. Cerami E, Gao J, Dogrusoz U, Gross BE, Sumer SO, Aksoy BA, Jacobsen A, Byrne CJ, Heuer ML, Larsson E, Antipin Y, Reva B, Goldberg AP, Sander C, Schultz N. The cBio Cancer Genomics Portal: an open platform for exploring multidimensional cancer genomics data. Cancer Discov. 2012;2:401–4.
46. Gao J, Aksoy BA, Dogrusoz U, Dresdner G, Gross B, Sumer SO, Sun Y, Jacobsen A, Sinha R, Larsson E, Cerami E, Sander C, Schultz N. Integrative analysis of complex cancer genomics and clinical profiles using the cBioPortal. Sci Signal. 2013;6:pl1.
47. Liu X, Ory V, Chapman S, Yuan H, Albanese C, Kallakury B, Timofeeva OA, Nealon C, Dakic A, Simic V, Haddad BR, Rhim JS, Dritschilo A, Riegel A, McBride A, Schlegel R. ROCK inhibitor and feeder cells induce the conditional reprogramming of epithelial cells. Am J Pathol. 2012;180:599–607.
48. Ben-Porath I, Thomson MW, Carey VJ, Ge R, Bell GW, Regev A, Weinberg RA. An embryonic stem cell-like gene expression signature in poorly differentiated aggressive human tumors. Nat Genet. 2008;40:499–507.
49. Vogelstein B, Papadopoulos N, Velculescu VE, Zhou S, Diaz Jr LA, Kinzler KW. Cancer genome landscapes. Science. 2013;339:1546–58.
50. Tamborero D, Gonzalez-Perez A, Perez-llamas C, Deu-Pons J, Kandoth C, Reimand J, Lawrence MS, Getz G, Bader GD, Ding L, Lopez-Bigas N. Comprehensive identification of mutational cancer driver genes across 12 tumor types. Sci Rep. 2013;3:2650.
51. Lawrence MS, Stojanov P, Mermel CH, Robinson JT, Garraway LA, Golub TR, Meyerson M, Gabriel SB, Lander ES, Getz G. Discovery and saturation analysis of cancer genes across 21 tumour types. Nature. 2014;505:495–501.
52. Yeo G, Burge CB. Maximum entropy modeling of short sequence motifs with applications to RNA splicing signals. J Comput Biol. 2004;11:377–94.
53. Lawrence MS, Stojanov P, Polak P, Kryukov GV, Cibulskis K, Sivachenko A, Carter SL, Stewart C, Mermel CH, Roberts S a, Kiezun A, Hammerman PS, McKenna A, Drier Y, Zou L, Ramos AH, Pugh TJ, Stransky N, Helman E, Kim J, Sougnez C, Ambrogio L, Nickerson E, Shefler E, Cortés ML, Auclair D, Saksena G, Voet D, Noble M, DiCara D, et al. Mutational heterogeneity in cancer and the search for new cancer-associated genes. Nature. 2013;499:214–8.
54. Silber J, Lim DA, Petritsch C, Persson AI, Maunakea AK, Yu M, Vandenberg SR, Ginzinger DG, James CD, Costello JF, Bergers G, Weiss WA, Alvarez-Buylla A, Hodgson JG. miR-124 and miR-137 inhibit proliferation of glioblastoma multiforme cells and induce differentiation of brain tumor stem cells. BMC Med. 2008;6:14.
55. Yang L. miR-124 inhibits the growth of glioblastoma through the downregulation of SOS1. Mol Med Rep. 2013;8:345–9.
56. Chen Q, Lu G, Cai Y, Li Y, Xu R, Ke Y, Zhang S. MiR-124-5p inhibits the growth of high-grade gliomas through posttranscriptional regulation of LAMB1. Neuro Oncol. 2014;16:637–51.
57. Cai J-J, Qi Z-X, Chen L-C, Yao Y, Gong Y, Mao Y. miR-124 suppresses the migration and invasion of glioma cells in vitro via Capn4. Oncol Rep. 2016;35:284–90.
58. Bahrami-Samani E, Vo DT, de Araujo PR, Vogel C, Smith AD, Penalva LOF, Uren PJ. Computational challenges, tools, and resources for analyzing co- and post-transcriptional events in high throughput. Wiley Interdiscip Rev RNA. 2015;6:291–310.
59. Tsai YS, Dominguez D, Gomez SM, Wang Z. Transcriptome-wide identification and study of cancer-specific splicing events across multiple tumors. Oncotarget. 2015;6:6825–39.
60. Sebestyén E, Zawisza M, Eyras E, Zawisza M. Recurrent alternative splicing isoform switches in tumor samples provide novel signatures of cancer. Nucleic Acids Res. 2015;43:1345–56.
61. Dvinge H, Bradley RK. Widespread intron retention diversifies most cancer transcriptomes. Genome Med. 2015;7:1–13.
62. Chesnais V, Kosmider O, Damm F, Itzykson R, Bernard OA, Solary E, Fontenay M. Spliceosome mutations in myelodysplastic syndromes and chronic myelomonocytic leukemia. Oncotarget. 2012;3:1284–93.
63. Ramsay AJ, Martínez-Trillos A, Jares P, Rodríguez D, Kwarciak A, Quesada V. Next-generation sequencing reveals the secrets of the chronic lymphocytic leukemia genome. Clin Transl Oncol. 2013;15:3–8.
64. Scott LM, Rebel VI. Acquired mutations that affect pre-mRNA splicing in hematologic malignancies and solid tumors. J Natl Cancer Inst. 2013;105:1540–9.
65. Zhang J, Manley JL. Misregulation of pre-mRNA alternative splicing in cancer. Cancer Discov. 2013;3:1228–37.
66. Jin DI, Lee SW, Han ME, Kim HJ, Seo SA, Hur GY, Jung S, Kim BS, Oh SO. Expression and roles of Wilms' tumor 1-associating protein in glioblastoma. Cancer Sci. 2012;103:2102–9.
67. Ferrarese R, Harsh IV GR, Yadav AK, Bug E, Maticzka D, Reichardt W, Dombrowski SM, Miller TE, Masilamani AP, Dai F, Kim H, Hadler M, Scholtens DM, Yu ILY, Beck J, Srinivasasainagendra V, Costa F, Baxan N, Pfeifer D, Von Elverfeldt D, Backofen R, Weyerbrock A, Duarte CW, He X, Prinz M, Chandler JP, Vogel H, Chakravarti A, Rich JN, Carro MS, et al. Lineage-specific splicing of a brain-enriched alternative exon promotes glioblastoma progression. J Clin Invest. 2014;124:2861–76.
68. Lo H-W, Zhu H, Cao X, Aldrich A, Ali-Osman F. A novel splice variant of GLI1 that promotes glioblastoma cell migration and invasion. Cancer Res. 2009;69:6790–8.
69. Hirvonen HE, Salonen R, Sandberg MM, Vuorio E, Västrik I, Kotilainen E, Kalimo H. Differential expression of myc, max and RB1 genes in human gliomas and glioma cell lines. Br J Cancer. 1994;69:16–25.
70. Camacho-Vanegas O, Narla G, Teixeira MS, DiFeo A, Misra A, Singh G, Chan AM, Friedman SL, Feuerstein BG, Martignetti JA. Functional inactivation of the KLF6 tumor suppressor gene by loss of heterozygosity and increased alternative splicing in glioblastoma. Int J Cancer. 2007;121:1390–5.
71. Chan YA, Hieter P, Stirling PC. Mechanisms of genome instability induced by RNA processing defects. Trends Genet. 2014;30:245–53.
72. Papasaikas P, Tejedor JR, Vigevani L, Valcárcel J. Functional splicing network reveals extensive regulatory potential of the core spliceosomal machinery. Mol Cell. 2015;57:7–22.
73. Saltzman AL, Pan Q, Blencowe BJ. Regulation of alternative splicing by the core spliceosomal machinery. Genes Dev. 2011;25:373–84.
74. Wang Z, Murigneux V, Le Hir H. Transcriptome-wide modulation of splicing by the exon junction complex. Genome Biol. 2014;15:1–18.
75. Shao C, Yang B, Wu T, Huang J, Tang P, Zhou Y, Zhou J, Qiu J, Jiang L, Li H, Chen G, Sun H, Zhang Y, Denise A, Zhang D-E, Fu X-D. Mechanisms for U2AF to define 3′ splice sites and regulate alternative splicing in the human genome. Nat Struct Mol Biol. 2014;21:997–1005.
76. Lynch DC, Revil T, Schwartzentruber J, Bhoj EJ, Innes AM, Lamont RE, Lemire EG, Chodirker BN, Taylor JP, Zackai EH, McLeod DR, Kirk EP, Hoover-Fong J, Fleming L, Savarirayan R, Majewski J, Jerome-Majewska L a, Parboosingh JS, Bernier FP. Disrupted auto-regulation of the spliceosomal gene SNRPB causes cerebro-costo-mandibular syndrome. Nat Commun. 2014;5:4483.
77. Bacrot S, Doyard M, Huber C, Alibeu O, Feldhahn N, Lehalle D, Lacombe D, Marlin S, Nitschke P, Petit F, Vazquez M-P, Munnich A, Cormier-Daire V. Mutations in *SNRPB*, encoding components of the core splicing machinery, cause cerebro-costo-mandibular syndrome. Hum Mutat. 2015;36:187–90.

78. Lehalle D, Wieczorek D, Zechi-Ceide RM, Passos-Bueno MR, Lyonnet S, Amiel J, Gordon CT. A review of craniofacial disorders caused by spliceosomal defects. Clin Genet. 2015;88:405–15.
79. Kittler R, Putz G, Pelletier L, Poser I, Heninger A-K, Drechsel D, Fischer S, Konstantinova I, Habermann B, Grabner H, Yaspo M-L, Himmelbauer H, Korn B, Neugebauer K, Pisabarro MT, Buchholz F. An endoribonuclease-prepared siRNA screen in human cells identifies genes essential for cell division. Nature. 2004;432:1036–40.
80. Valles I, Pajares MJ, Segura V, Guruceaga E, Gomez-Roman J, Blanco D, Tamura A, Montuenga LM, Pio R. Identification of novel deregulated RNA metabolism-related genes in non-small cell lung cancer. PLoS One. 2012;7:e42086.
81. Yi Y, Nandana S, Case T, Nelson C, Radmilovic T, Matusik RJ, Tsuchiya KD. Candidate metastasis suppressor genes uncovered by array comparative genomic hybridization in a mouse allograft model of prostate cancer. Mol Cytogenet. 2009;2:18.
82. Romero A, García-García F, López-Perolio I. Ruiz de Garibay G, García-Sáenz JA, Garre P, Ayllón P, Benito E, Dopazo J, Díaz-Rubio E, Caldés T, de la Hoya M. BRCA1 Alternative splicing landscape in breast tissue samples. BMC Cancer. 2015;15:1–8.
83. Li L, Cohen M, Wu J, Sow MH, Nikolic B, Bischof P, Irminger-Finger I. Identification of BARD1 splice-isoforms involved in human trophoblast invasion. Int J Biochem Cell Biol. 2007;39:1659–72.
84. Lastella P, Surdo N, Resta N, Guanti G, Stella A. In silico and in vivo splicing analysis of MLH1 and MSH2 missense mutations shows exon- and tissue-specific effects. BMC Genomics. 2006;7:243.
85. Kim KK, Shin BA, Seo KH, Kim PN, Koh JT, Kim JH, Park BR. Molecular cloning and characterization of splice variants of human RAD50 gene. Gene. 1999; 235:59–67.
86. Pabla N, Bhatt K, Dong Z. Checkpoint kinase 1 (Chk1)-short is a splice variant and endogenous inhibitor of Chk1 that regulates cell cycle and DNA damage checkpoints. Proc Natl Acad Sci. 2012;109:197–202.
87. The Cancer Genome Atlas. [http://cancergenome.nih.gov/].
88. CGHub: The Cancer Genomics Hub. [https://cghub.ucsc.edu/].
89. SRA: Sequence Read Archive. [http://www.ncbi.nlm.nih.gov/sra].
90. UCSC Genome Browser. [https://genome.ucsc.edu/].
91. Wu TD, Nacu S. Fast and SNP-tolerant detection of complex variants and splicing in short reads. Bioinformatics. 2010;26:873–81.
92. Li H, Handsaker B, Wysoker A, Fennell T, Ruan J, Homer N, Marth G, Abecasis G, Durbin R. The Sequence Alignment/Map format and SAMtools. Bioinformatics. 2009;25:2078–9.
93. Anders S, Pyl PT, Huber W. HTSeq–a Python framework to work with high-throughput sequencing data. Bioinformatics. 2015;31:166–9.
94. Love MI, Huber W, Anders S. Moderated estimation of fold change and dispersion for RNA-seq data with DESeq2. Genome Biol. 2014;15:550.
95. Gautier L, Cope L, Bolstad BM, Irizarry RA. Affy - analysis of Affymetrix GeneChip data at the probe level. Bioinformatics. 2004;20:307–15.
96. Ritchie ME, Phipson B, Wu D, Hu Y, Law CW, Shi W, Smyth GK. Limma powers differential expression analyses for RNA-sequencing and microarray studies. Nucleic Acids Res. 2015;43:e47–7.
97. Jacobsen A. CDGS-R Package - R-based API for accessing the MSKCC Cancer Genomics Data Server (CGDS). 2015. [http://www.cbioportal.org/cgds_r.jsp].
98. Chou C-H, Chang N-W, Shrestha S, Hsu S-D, Lin Y-L, Lee W-H, Yang C-D, Hong H-C, Wei T-Y, Tu S-J, Tsai T-R, Ho S-Y, Jian T-Y, Wu H-Y, Chen P-R, Lin N-C, Huang H-T, Yang T-L, Pai C-Y, Tai C-S, Chen W-L, Huang C-Y, Liu C-C, Weng S-L, Liao K-W, Hsu W-L, Huang H-D. miRTarBase 2016: updates to the experimentally validated miRNA-target interactions database. Nucleic Acids Res. 2016;2016(44):D239–47.
99. Dennis G, Sherman BT, Hosack DA, Yang J, Gao W, Lane H, Lempicki RA. DAVID: database for annotation, visualization, and integrated discovery. Genome Biol. 2003;4:R60.
100. Supek F, Bošnjak M, Škunca N, Šmuc T. REVIGO summarizes and visualizes long lists of gene ontology terms. PLoS One. 2011;6:e21800.
101. Shannon P. Cytoscape: A software environment for integrated models of biomolecular interaction networks. Genome Res. 2003;13:2498–504.
102. HomoloGene. [http://www.ncbi.nlm.nih.gov/homologene].
103. Shen S, Park JW, Huang J, Dittmar KA, Lu ZX, Zhou Q, Carstens RP, Xing Y . MATS: a Bayesian framework for flexible detection of differential alternative splicing from RNA-Seq data. Nucleic Acids Res. 2012;40:1–13.
104. Shen S, Park JW, Lu Z, Lin L, Henry MD, Wu YN, Zhou Q, Xing Y. rMATS: Robust and flexible detection of differential alternative splicing from replicate RNA-Seq data. Proc Natl Acad Sci. 2014;111:E5593–601.
105. R Project. [http://www.r-project.org/].
106. Krzywinski M, Schein J, Birol I, Connors J, Gascoyne R, Horsman D, Jones SJ, Marra MA. Circos: an information aesthetic for comparative genomics. Genome Res. 2009;19:1639–45.
107. Katz Y, Wang ET, Stilterra J, Schwartz S, Wong B, Thorvaldsdottir H, Robinson JT, Mesirov JP, Airoldi EM, Burge CB. Sashimi plots: quantitative visualization of alternative isoform expression from RNA-seq data. Bioinformatics. 2015;31:2400–2.
108. Inkscape. [https://inkscape.org/].
109. European Nucleotide Archive - ENA. [http://www.ebi.ac.uk/ena]
110. Jijiwa M, Demir H, Gupta S, Leung C, Joshi K, Orozco N, Huang T, Yildiz VO, Shibahara I, de Jesus JA, Yong WH, Mischel PS, Fernandez S, Kornblum HI, Nakano I. CD44v6 regulates growth of brain tumor stem cells partially through the AKT-mediated pathway. PLoS One. 2011;6:e24217.
111. Guvenc H, Pavlyukov MS, Joshi K, Kurt H, Banasavadi-Siddegowda YK, Mao P, Hong C, Yamada R, Kwon C-H, Bhasin D, Chettiar S, Kitange G, Park I-H, Sarkaria JN, Li C, Shakhparonov MI, Nakano I. Impairment of glioma stem cell survival and growth by a novel inhibitor for survivin-ran protein complex. Clin Cancer Res. 2013;19:631–42.
112. Nakano I, Masterman-Smith M, Saigusa K, Paucar AA, Horvath S, Shoemaker L, Watanabe M, Negro A, Bajpai R, Howes A, Lelievre V, Waschek JA, Lazareff JA, Freije WA, Liau LM, Gilbertson RJ, Cloughesy TF, Geschwind DH, Nelson SF, Mischel PS, Terskikh A V, Kornblum HI. Maternal embryonic leucine zipper kinase is a key regulator of the proliferation of malignant brain tumors, including brain tumor stem cells. J Neurosci Res. 2008;86:48–60.
113. Dougherty JD, Garcia ADR, Nakano I, Livingstone M, Norris B, Polakiewicz R, Wexler EM, Sofroniew M V, Kornblum HI, Geschwind DH. PBK/TOPK, a proliferating neural progenitor-specific mitogen-activated protein kinase kinase. J Neurosci. 2005;25:10773–85.
114. Will CL, Lührmann R. Spliceosome structure and function. Cold Spring Harb Perspect Biol. 2011;3:1–2.